

EXACT CLASSIFICATION OF NMR SPECTRA FROM NMR SIGNALS

Pedro Izquierdo Lehmann*, Aline Xavier[†], Marcelo E. Andia[†], Carlos A. Sing Long^{†*}

*Johns Hopkins University, [†]Universidad de Santiago de Chile,
[†]Pontificia Universidad Católica de Chile

ABSTRACT

Nuclear magnetic resonance (NMR) spectroscopy is routinely used to study the properties of matter. Therefore, different materials can be classified according to their NMR spectra. However, the NMR spectra cannot be observed directly, and only the NMR signal, which is a sum of complex exponentials, is directly observable in practice. A popular approach to recover the spectrum is to perform harmonic retrieval, i.e., to reconstruct exactly the spectrum from the NMR signal. However, even when this approach fails, the spectrum might still be classified accurately. In this work, we model the spectrum as an atomic measure to study the performance of classifying the spectrum from the NMR signal, and to determine how it degrades in the presence of additive noise and changes in field intensity. Although we focus on NMR signals, our results are broadly applicable to sum-of-exponential signals. We show numerical results illustrating our claims.

Index Terms— Sum of exponentials, harmonic signals, nuclear magnetic resonance spectroscopy, magnetic resonance spectroscopy, signal classification, end-to-end classification, harmonic retrieval.

1. INTRODUCTION

Nuclear magnetic resonance (NMR) spectroscopy is a widely used technique to investigate dynamically the physical, chemical and biological properties of matter [1]. In an NMR experiment a sample is plunged into an intense *external magnetic field*, and excited with radiofrequency electromagnetic waves. The signal generated by this experiment, called *free induction decay* or simply the *NMR signal*, corresponds to a *sum-of-exponentials*

$$u(t) = \sum_k c_k e^{\lambda_k t} \quad (1)$$

where the complex exponents $\{\lambda_k\}$ determine the oscillation frequency and the rate of decay of each term, and the

*M.E.A. was partially funded by ANID - Fondecyt - 1220922. P.I.L. and M.E.A. were partially funded by ANID - Millennium Science Initiative Program - ICN2021.004. P.I.L. and C.SL. were partially funded by grant ANID - Fondecyt - 1211643. C.SL. was partially funded by grant CENIA - FB210017 - Basal - ANID.

weights $\{c_k\}$ determine their amplitude and phase. The imaginary part of the exponents determines the *NMR spectrum* of the sample, and it reveals information about its constitutive materials. For this reason, NMR spectroscopy is routinely used in a broad range of applications. For example, NMR spectroscopy has been shown to be useful in studying liver diseases by quantifying the relative concentration of fatty acids [2].

As the NMR spectrum contains detailed information about the composition of a sample, it can reveal whether the sample exhibits a specific set of properties. In other words, we can *classify* the sample into different categories using its NMR spectrum. For example, the NMR spectrum has the potential to reveal early stages of liver disease [2, 3], allowing for its early diagnosis. However, the spectrum cannot be measured directly, but only indirectly through the NMR signal (1) measured in an experiment.

For this reason, a traditional approach to classify the spectrum is to perform *harmonic retrieval (HR)*, that is, to attempt to recover exactly the exponents and the weights from the signal u to then classify these values. There is an extensive literature devoted to the development and implementation of methods for HR, such as Prony-like methods [4], matrix pencil methods [5], MUSIC [6], total variation (TV) minimization methods [7], atomic norm minimization methods [8], parameter estimation using optimization [9] and, more recently, deep learning methods [10]. Although these methods work well in practice, there are limits to the amount of information that can be retrieved. For instance, when two exponents are too close to each other, the sampling rate required to accurately recover both increases substantially. Furthermore, the methods themselves often become unstable in the presence of noise [11].

Since the NMR signal encodes information about the sample, it may still be possible to classify the spectrum directly from the NMR signal [12] even when HR may fail. This strategy has become increasingly popular due to the advent of *end-to-end Machine Learning (ML)* [13] for classifying NMR signals [14], and, from a theoretical standpoint, due to the fact that the conditions for exact classification of the NMR spectrum should be less constraining than those for which HR is successful. However, there are open questions regarding the performance and the limitations of these strategies, which, as

is the case for HR, are closely related to the structure of the NMR spectrum. Furthermore, the response may be corrupted by additive noise, impacting the performance of any classification method on the NMR signal.

In this work we assume that the classes of NMR spectra are disjoint, and we develop a model based on atomic measures in the complex plane to determine when the NMR spectrum can be classified only from its associated NMR signal. In particular, we are interested in the effect of the field intensity, which impacts the decay of the signal, on the classification performance. Furthermore, we study the impact of additive noise on the NMR signal in the classification. We present experiments to illustrate our theoretical results.

2. MATHEMATICAL MODEL

2.1. The spectrum

We represent the *spectrum* $\{(c_k, \lambda_k)\}$ of a sample as a complex measure on \mathbb{C}

$$\mu = \sum_{k=1}^p c_k \delta_{\lambda_k} \quad (2)$$

where $\{\lambda_k\}_{k=1}^p$ and $\{c_k\}_{k=1}^p$ are the exponents and weights of the signal in (1) and p is finite, but otherwise arbitrary. Remark that this is the measure associated to the NMR signal in (1) and is different from the *NMR spectrum*, which typically refers *only* to $\{(|c_k|, \text{Im}(\lambda_k))\}$.

Since the NMR signal decays in time, the real part of the exponents is negative. Hence, we assume that there exist $\gamma_-, \gamma_+ \in \mathbb{R}_+$ such that $\gamma_- \leq -\text{Re}(\lambda_k) \leq \gamma_+$ for each k . These constants bound the minimum and maximum decaying rates of the components of the NMR signal. Therefore, we define

$$\mathcal{S}_p := \left\{ \sum_{k=1}^p c_k \delta_{\lambda_k} : \gamma_- \leq -\text{Re}(\lambda_k) \leq \gamma_+, c_k \in \mathbb{C} \right\}.$$

The spectrum of a system is then represented by a measure in \mathcal{S}_p . The magnitude is quantified by its *total variation*

$$\|\mu\|_{\text{TV}} = \sup_{f \in C^0(\mathbb{C}) : |f| \leq 1} \int_{\mathbb{C}} f(z) d\mu(z).$$

We assume that all the measures in this work have finite total variation. Observe that when the measure is atomic as in (2) then $\|\mu\|_{\text{TV}} = \sum_{k=1}^p |c_k|$.

2.2. The NMR signal

From (2) we can represent the NMR signal in (1) as the integral transform

$$u(t) = S\mu(t) := \int_{\mathbb{C}} e^{\lambda t} d\mu(\lambda) \quad (3)$$

of the measure μ . Hence, we are led to a *linear* relation between u and μ . Furthermore, when $\mu \in \mathcal{S}_p$ the NMR signal has finite energy. From [15, Proposition 4.2.5]

$$|S\mu(t)| \leq \sum_{k=1}^p |c_k| e^{\text{Re}(\lambda_k)t} \leq e^{-\gamma_- t} \|\mu\|_{\text{TV}}$$

we deduce that $S\mu \in L^2(\mathbb{R}_+)$ with

$$\|S\mu\|_{L^2} \leq \|\mu\|_{\text{TV}} / \sqrt{2\gamma_-}. \quad (4)$$

Typically, the NMR signal is corrupted by noise. Hence, we also consider the additive noise model

$$v := u + w = S\mu + w \quad (5)$$

where $w \in L^2(\mathbb{R}_+)$ represents an unknown perturbation with L^2 -norm bounded by a known value $\sigma > 0$.

2.3. Classes of spectra

We assume that the spectra in \mathcal{S}_p associated to the properties of interest can be grouped in *classes* $O_1, \dots, O_N \subset \mathcal{S}_p$. Usually these classes are known, as they are determined by the properties being looked for in a sample, or by other considerations. A key assumption that we will make is that there is a fixed, but unknown, relation between the real and the imaginary part of the exponents of all the spectra in $O_1 \cup \dots \cup O_N$. Specifically, we suppose that there exists a function $\rho : \mathbb{R} \rightarrow \mathbb{R}$ such that $\gamma_- \leq -\rho \leq \gamma_+$ and $\lambda_k = -\rho(\omega_k) + i\omega_k$ for any $\mu \in O_1 \cup \dots \cup O_N$. In practice, this implies that the rate of decay of the terms in (1) depends *only* on the oscillation frequency. Hence, the classes O_i are differentiated only by their frequencies, that is, by their NMR spectra.

2.4. Classification of spectra

It is natural to assume that the classes $\{O_i\}_{i=1}^N$ are disjoint, so that no spectrum belongs to two distinct classes; we will further assume that if we measure the distance between them

$$\kappa_{\text{TV}}(O_i, O_j) := \inf\{\|\mu - \nu\|_{\text{TV}} : \mu \in O_i, \nu \in O_j\}$$

then $\kappa_{\text{TV}}(O_i, O_j) > 0$ when $i \neq j$. Although this implies that the spectra can be perfectly classified by *some* classifier, in practice the spectra cannot be observed directly. In contrast, the NMR signal associated to each spectrum can be observed. The set of NMR signals generated by the spectra in O_i is the set SO_i . We measure the distance between them as

$$\kappa_{L^2}(SO_i, SO_j) := \inf\{\|S\mu - S\nu\|_{L^2} : \mu \in O_i, \nu \in O_j\}.$$

If $\kappa_{L^2}(SO_i, SO_j) > 0$ when $i \neq j$ then any state can be perfectly classified from its NMR signal by *some* classifier. However, the map S may substantially reduce this distance in comparison to $\kappa_{\text{TV}}(O_i, O_j)$. This leads to an increased sensitivity to noise. The noise model (5) leads us to analyze

$$\inf_{\|w\|_{L^2} \leq \sigma, \|w'\|_{L^2} \leq \sigma} \kappa_{L^2}(SO_i + w, SO_j + w')$$

which might become arbitrarily small or zero. Hence, our goal is to compare these distances to $\kappa_{\text{TV}}(O_i, O_j)$ and to find conditions for perfect classification.

3. CLASSIFICATION OF STATES FROM NMR SIGNALS

The distortion introduced by S is quantified by constants $c_-, c_+ > 0$ such that

$$c_- \|\mu\|_{\text{TV}} \leq \|S\mu\|_{L^2} \leq c_+ \|\mu\|_{\text{TV}} \quad (6)$$

for any $\mu \in \mathcal{S}_p$. The arguments in Section 2.2 allow us to use $c_+ = 1/\sqrt{2\gamma_-}$. To find a suitable c_- note that

$$\|S\mu\|_{L^2}^2 = \int_0^\infty \left| \sum_{k=1}^p c_k e^{\lambda_k t} \right|^2 dt = \mathbf{c}^* \mathbf{G}(\mu) \mathbf{c}$$

where $\mathbf{G}(\mu)$ is the symmetric positive semidefinite matrix with entries

$$G_{k,\ell}(\mu) = \int_0^\infty e^{(\lambda_k^* + \lambda_\ell)t} dt = -(\lambda_k^* + \lambda_\ell)^{-1} \quad (7)$$

and \mathbf{c} is the vector of weights $\{c_k\}_{k=1}^p$. Hence, c_- can be bounded as long as we can bound the smallest eigenvalue of this matrix. Let

$$R_p := \left\lceil \frac{p-1}{2} \right\rceil, \quad H_p := 2 \sum_{m=1}^{R_p} m^{-1}.$$

The main result of this work is the following. We defer its proof to Section 7.

Theorem 3.1. Suppose that $p \geq 2$ and let $\mu \in \mathcal{S}_p$. If there exists $\Delta > 0$ such that

$$|\text{Im}(\lambda_k - \lambda_\ell)| \geq \Delta > 2\sqrt{H_p^2 \gamma_+^2 - p^{-2}(\gamma_+ + \gamma_-)^2} \quad (8)$$

then (6) holds with $c_- = \sqrt{\eta/p}$ for

$$\eta = \frac{1}{2\gamma_+} - \frac{H_p R_p}{\sqrt{(\gamma_+ + \gamma_-)^2 + \Delta^2 R_p^2}}.$$

Notice that if $\gamma_+ = \gamma_-$ and $p = 2$ then the lower bound in (8) is equal to 0. However, the bound becomes more restrictive as p or the range of uncertainty of the decay $\gamma_+ - \gamma_-$ increases. Theorem 3.1 leads to a bound on the distortion introduced by the map S .

Theorem 3.2. If every $\mu \in O_i - O_j$ satisfy (8) then

$$\sqrt{\frac{\eta}{2p}} \leq \frac{\kappa_{L^2}(SO_i, SO_j)}{\kappa_{\text{TV}}(O_i, O_j)} \leq \sqrt{\frac{1}{2\gamma_+}}.$$

Finally, from Theorem 3.2 follows a bound on the noise level σ for which we may still have perfect classification.

Corollary 3.1. If every $\mu \in O_i - O_j$ satisfy (8) then

$$\sigma < \sqrt{\eta/4p} \kappa_{\text{TV}}(O_i, O_j)$$

then there exists some exact classifier for the spectra using their NMR signal.

4. NUMERICAL EXPERIMENTS

To illustrate how representative are the bounds in practical applications, we use ^1H NMR spectroscopy data from fatty acid methyl ester (FAME) samples obtained using a 9.4 T Bruker Avance spectrometer. The data were acquired with the protocol Zg30 (30 degrees excitation pulse). For each NMR signal we measured a sample of fatty acids (FA) extracted from the liver of 12 mice with nonalcoholic steatohepatitis (NASH), and from 12 healthy mice from a control group.

The class of NMR signals from healthy mice is $C = \{u_1, \dots, u_{12}\}$ whereas the class for mice with NASH is $N = \{u_{13}, \dots, u_{24}\}$. Fig. 1a shows the spectrum of u_1 and u_{13} . Since the noise level is very low, we assume that for each k we have $u_k = S\mu_k$ for some measure $\mu_k \in \mathcal{S}_p$. We define O_C and O_N accordingly. By inspection, we estimate $p = 9$, $\Delta = 100$ Hz, and $\gamma_0 = 3.36529$ Hz as the average decay rate. We set $\gamma_- = 0.9\gamma_0$ and $\gamma_+ = 1.1\gamma_0$. That is, we assume that the decay rate of each of each term of the sum (1) is contained in $[\gamma_-, \gamma_+]$. For $\gamma \in \mathbb{R}_+$ we synthetize the NMR signals $u_k^\gamma(t) = e^{-\gamma t} u_k(t)$ and define the classes $C^\gamma = \{u_1^\gamma, \dots, u_{12}^\gamma\}$ and $N^\gamma = \{u_{13}^\gamma, \dots, u_{24}^\gamma\}$. By construction, $u_k^\gamma = S\mu_k^\gamma$, where μ_k^γ is equal to μ_k with its support shifted by $-\gamma$ on the complex plane; we define O_C^γ and O_N^γ accordingly. Thus, the latter satisfy the same separation condition as O_C and O_N .

We test the bounds of Theorem 3.2 by computing $E(\gamma) = \kappa_{L^2}(C^\gamma, N^\gamma)/\kappa_{\text{TV}}(O_C, O_N)$, $U(\gamma) = \sqrt{1/2(\gamma_+ + \gamma)}$ and $L(\gamma) = \sqrt{\eta(\gamma)/2p}$, where

$$\eta(\gamma) = \frac{1}{2(\gamma_+ + \gamma)} - \frac{H_p \lceil (p-1)/2 \rceil}{\sqrt{(\gamma_+ + \gamma_- + 2\gamma)^2 + \Delta^2 \lceil (p-1)/2 \rceil^2}}.$$

For this we consider $\gamma \in [\gamma_0, \gamma_1]$, where $\gamma_1 = 3.2\gamma_0$. In this experiment, we estimate

$$\kappa_{\text{TV}}(O_C, O_N) = \sqrt{2/9\gamma_0} \kappa_{L^2}(C, N).$$

The results can be seen in Fig. 1b.

5. DISCUSSION

Theorem 3.2 shows that classification robustness to additive noise degrades inversely proportional to the square root of the decay rates. This quantifies the impact of the well known fact that a large decay rate reduces the effective interval of observation for each one of the components of the NMR signal (1), making it challenging to distinguish low frequencies *unless* they are well separated.

Our results show the validity of the bounds in an experimental setting. While our upper bound always hold, our lower bound seem hold on a limited but practical range of decay rates. It is limited since the bound in (8) is increasing on the maximum decay rate γ_+ and when $\gamma_- \ll 1$ the leading term is $\approx 2(H_p - p^{-2})^{1/2}\gamma_+$; for $p = 10$ we have $\approx 20\gamma_+$. On

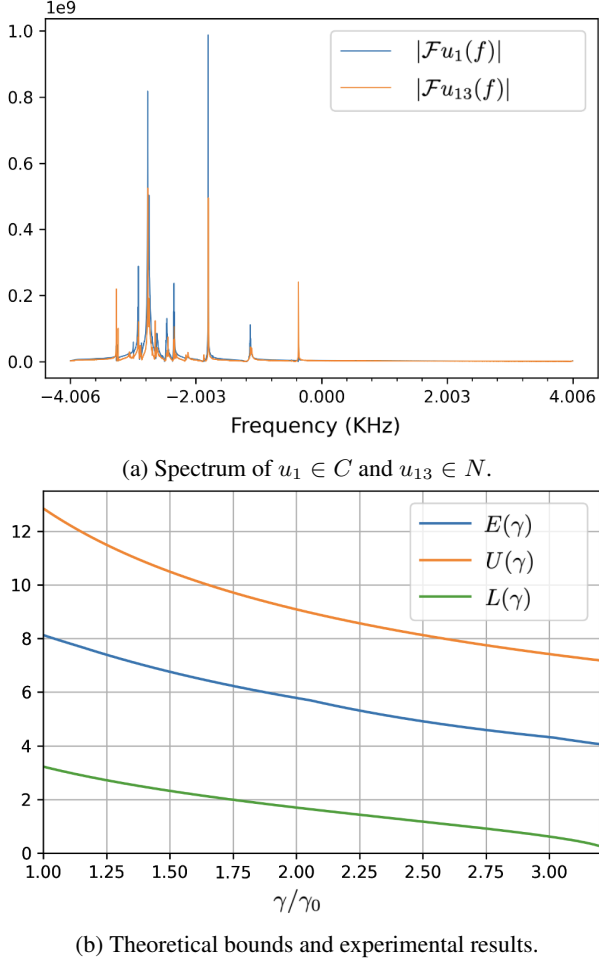


Fig. 1: Experimental results

the other side, since the decay rate in NMR spectroscopy depends on the magnetic field, the range of validity of our bound is practical in that it reflects a potential reduction of the external field from 9.4 T to 3 T. Consequently, the NMR spectra can be classified from NMR signals at 9.4 T and 3 T.

6. CONCLUSIONS

We develop a model based on atomic measures in the complex plane that allows us to study when the NMR spectrum can be classified only from its associated NMR signal. Our theoretical results provide a frequency separation condition that is inversely proportional to the decay rate, i.e. the intensity of the external magnetic field, which ensure that the NMR spectrum can be classified directly from its associated NMR signal as long as the SNR of the NMR signal is proportional to the square root of this external field. Our experiments show that the bounds we obtained are valid over a range of decay rates of the NMR signal that may represent a large factor of variation of the system parameters, e.g. external field.

7. PROOF OF MAIN RESULTS

Proof of Theorem 3.1. The entries in (7) depend only on $\lambda_1, \dots, \lambda_p$. By definition they are all distinct. Write $\lambda_k = -a_k + ib_k$ with $a_k \geq 0$. Then, by Lemma 7.1 and Lemma 7.2 we have

$$\begin{aligned} & (-2 \operatorname{Re}(\lambda_k))^{-1} - \sum_{\ell \neq k} |\lambda_k^* + \lambda_\ell|^{-1} \\ &= (2a_k)^{-1} - \sum_{\ell \neq k} \sqrt{(a_k + a_\ell)^2 + (b_k - b_\ell)^2}^{-1} \\ &\geq (2a_k)^{-1} - \sum_{\ell \neq k} \sqrt{(a_k + \gamma_-)^2 + (b_k - b_\ell)^2}^{-1} \\ &\geq (2a_k)^{-1} - 2 \sum_{m=1}^{\lceil p-1 \rceil} \sqrt{(a_k + \gamma_-)^2 + (m\Delta)^2}^{-1} \\ &\geq (2a_k)^{-1} - H_p \sqrt{\left(\frac{a_k + \gamma_-}{\lceil (p-1)/2 \rceil} \right)^2 + \Delta^2}^{-1} \\ &\geq (2\gamma_+)^{-1} - H_p \sqrt{\left(\frac{\gamma_+ + \gamma_-}{\lceil (p-1)/2 \rceil} \right)^2 + \Delta^2}^{-1}. \end{aligned}$$

Hence, $\mathbf{G}(\mu)$ is diagonally dominant. Its smallest eigenvalue is bounded below by η uniformly in the weights of μ . It follows from the hypothesis that $\eta > 0$. Thus,

$$\mathbf{c}^\top \mathbf{G}(\mu) \mathbf{c} \geq \eta \|\mathbf{c}\|_2^2 \geq (\eta/p) \|\mathbf{c}\|_1^2 = (\eta/p) \|\mu\|_{\text{TV}}^2.$$

□

Proof of Theorem 3.2. Let $O_{i,j} = O_i \times O_j$. If $\mu, \nu \in \mathcal{S}_p$ then $\mu - \nu \in \mathcal{S}_{2p}$. From (4) and Theorem 3.1 we have that

$$\begin{aligned} & (\eta/\sqrt{2p}) \kappa_{\text{TV}}(O_i, O_j) \\ &= \inf \{(\eta/\sqrt{2p}) \|\mu - \nu\|_{\text{TV}} : (\mu, \nu) \in O_{i,j}\} \\ &\leq \inf \{\|S(\mu - \nu)\|_{L^2} : (\mu, \nu) \in O_{i,j}\} \\ &\leq \inf \{\|\mu - \nu\|_{\text{TV}} : (\mu, \nu) \in O_{i,j}\} / \sqrt{2\gamma_-} \\ &= \kappa_{\text{TV}}(O_i, O_j) / \sqrt{2\gamma_-}. \end{aligned}$$

□

We present the following auxiliary lemmas. We omit their proof for brevity.

Lemma 7.1. *Let $f : \mathbb{R}_+ \rightarrow \mathbb{R}$ be decreasing, let $\Delta \geq 0$, and consider the problem*

$$\max_{t_1, \dots, t_p} \quad \sum_{k=1}^p f(|t_k|) \quad \text{s.t.} \quad |t_k| \geq \Delta, \quad |t_k - t_\ell| \geq \Delta.$$

An optimal solution is given by $t_k = (-1)^k \lceil k/2 \rceil \Delta$ and the optimal value is bounded from above by

$$2 \sum_{k=1}^{\lceil p-1 \rceil} f(k\Delta).$$

Lemma 7.2. *Let $b \geq 1$, $c, d \in \mathbb{R}$. Define $f : \mathbb{R}_+ \rightarrow \mathbb{R}$ as*

$$f(t) = t^{-1} - b \sqrt{(t+c)^2 + d^2}^{-1}.$$

Then $f'(t) \leq 0$ if $f(t) \geq 0$.

8. REFERENCES

- [1] Thomas C. Pochapsky and Susan Sondej Pochapsky, *NMR for Physical and Biological Scientists*, Garland Science, 1 edition, June 2006.
- [2] Aline Xavier, Flavia Zaconi, Constanza Gainza, Daniel Cabrera, Marco Arrese, Sergio Uribe, Carlos Sing-Long, and Marcelo E. Andia, “Intrahepatic fatty acids composition as a biomarker of NAFLD progression from steatosis to NASH by using ^1H -MRS,” *RSC Advances*, vol. 9, no. 72, pp. 42132–42139, 2019.
- [3] Begoña Lavin, Thomas R. Eykyn, Alkystis Phinikaridou, Aline Xavier, Shravan Kumar, Xabier Buqué, Patricia Aspichueta, Carlos Sing-Long, Marco Arrese, René M. Botnar, and Marcelo E. Andia, “Characterization of hepatic fatty acids using magnetic resonance spectroscopy for the assessment of treatment response to metformin in an eNOS $^+$ mouse model of metabolic nonalcoholic fatty liver disease/nonalcoholic steatohepatitis,” *NMR in Biomedicine*, p. e4932, Apr. 2023.
- [4] Riche Prony, “Essai expérimental et analytique: sur les lois de la dilatabilité de fluides élastique et sur celles de la force expansive de la vapeur de l’alkool, à différentes températures,” *Journal de l’École Polytechnique Floréal et Plairial, an III*, vol. 1, no. 22, pp. 24–76, 1975.
- [5] Y. Hua and T.K. Sarkar, “Matrix pencil method for estimating parameters of exponentially damped/undamped sinusoids in noise,” *IEEE Transactions on Acoustics, Speech, and Signal Processing*, vol. 38, no. 5, pp. 814–824, May 1990.
- [6] R. Schmidt, “Multiple emitter location and signal parameter estimation,” *IEEE Transactions on Antennas and Propagation*, vol. 34, no. 3, pp. 276–280, Mar. 1986.
- [7] Brett Bernstein, Sheng Liu, Chrysa Papadaniil, and Carlos Fernandez-Granda, “Sparse Recovery Beyond Compressed Sensing: Separable Nonlinear Inverse Problems,” *IEEE Transactions on Information Theory*, vol. 66, no. 9, pp. 5904–5926, Sept. 2020.
- [8] Dehui Yang, Gongguo Tang, and Michael B. Wakin, “Super-Resolution of Complex Exponentials From Modulations With Unknown Waveforms,” *IEEE Transactions on Information Theory*, vol. 62, no. 10, pp. 5809–5830, Oct. 2016.
- [9] Jeffrey M. Hokanson, “Projected Nonlinear Least Squares for Exponential Fitting,” *SIAM Journal on Scientific Computing*, vol. 39, no. 6, pp. A3107–A3128, Jan. 2017.
- [10] N. Schmid, S. Bruderer, F. Paruzzo, G. Fischetti, G. Toscano, D. Graf, M. Fey, A. Henrici, V. Ziebart, B. Heitmann, H. Grabner, J.D. Wegner, R.K.O. Sigel, and D. Wilhelm, “Deconvolution of 1D NMR spectra: A deep learning-based approach,” *Journal of Magnetic Resonance*, vol. 347, pp. 107357, Feb. 2023.
- [11] A. J. Barabell, J. Capon, D. F. DeLong, J. R. Johnson, and K. D. Senne, “Performance Comparison of Superresolution Array Processing Algorithms. Revised,” Tech. Rep. TST-72, Lincoln Laboratory, Lexington, Massachusetts, June 1998.
- [12] Magdalena Bouza, Andres Altieri, and Cecilia G. Galarza, “Classification of sums of complex exponentials,” 2021, Publisher: arXiv Version Number: 1.
- [13] Tobias Glassmachers, “Limits of End-to-End Learning,” in *Proceedings of Machine Learning Research*, 2017, vol. 77, pp. 17–32.
- [14] Carlos Cobas, “NMR signal processing, prediction, and structure verification with machine learning techniques,” *Magnetic Resonance in Chemistry*, vol. 58, no. 6, pp. 512–519, June 2020.
- [15] Donald L. Cohn, *Measure Theory: Second Edition*, Birkhäuser Advanced Texts Basler Lehrbücher. Springer New York, New York, NY, 2013.